

MORPHOLOGICAL COLOR PROCESSING BASED ON DISTANCES. APPLICATION TO COLOR DENOISING AND ENHANCEMENT BY CENTRE AND CONTRAST OPERATORS

Jesús Angulo

Centre de Morphologie Mathématique - Ecole des Mines de Paris,
35, rue Saint-Honoré, 77305 Fontainebleau, FRANCE
angulo@cmm.ensmp.fr ;http://cmm.ensmp.fr/~angulo

ABSTRACT

The extension of mathematical morphology operators to multi-valued functions, and in particular to color images, is neither direct nor general. In this paper is proposed a generalisation of distance-based and lexicographical-based approaches, allowing the extension of morphological operators to color images for any color representation (e.g. RGB, LSH and $L^*a^*b^*$) and for any metric distance to a reference color. The performance of these morphological color operators is illustrated by means of two applications: color denoising by the centre operator and color enhancement by the contrast mapping.

KEY WORDS

color mathematical morphology, color distance, vectorial ordering, noise removal, contrast enhancement, LSH, $L^*a^*b^*$

1 Introduction

Mathematical morphology is the application of lattice theory to spatial structures [12], in practice, the definition of morphological operators needs a totally ordered complete lattice structure, i.e., the possibility of defining an ordering relationship between the points to be processed. Therefore, the application of mathematical morphology to color images is difficult due to the vectorial nature of the color data. Fundamental references to works which have formalised the vector morphology theory are [14] [4] [17]. In the literature, many techniques have been proposed on the extension of mathematical morphology to color images according to different orderings. The marginal ordering or M-ordering is an ordering based on the usual pointwise ordering (i.e., component by component independently). Another more interesting one is called conditional ordering or C-ordering, where the vectors are ordered by means of some marginal components selected sequentially according to different conditions (i.e. lexicographic ordering). The reduced ordering or R-ordering performs the ordering of vectors according to some scalars, computed from the components of each vector with respect to different measure criteria, typically distances or projections. Using a M-ordering, we can introduce color vector values in the

transformed image that are not present in the input image (“false colors”) [14]. The application of a C-ordering a R-ordering preserves the input color vectors and therefore are preferable for filtering applications. The C-ordering has been widely studied in the framework of color morphology, especially in a luminance/saturation/hue representation [9] [17] [5] [2]. The R-ordering has been used to define morphological operators by means of distances in [4]. In [11] was proposed a combination of a R-ordering and a C-ordering, in fact our approach can be considered as a generalisation of this interesting study.

The aim of the first part of the paper is just to generalise the distance-based approaches and the lexicographical approaches in order to propose a general framework allowing the extension of morphological operators to color images for any color representation and for any metric distance. In fact, we introduce a generalisation of mathematical morphology to multivariate functions according to a distance-to-origin-based interpretation of the notion of total ordering between the points of a complete lattice. In the second part of this study is considered the application of morphological color operators to enhancement and denoising color images by means of two classical evolved operators: the morphological centre and the contrast mapping.

2 Preliminaries

2.1 Norms and distances

Given a n -dimensional vector $\mathbf{x} = (x_1 x_2 \dots x_n)$, $\mathbf{x} \in \mathbb{C}^n$ or $\in \mathbb{R}^n$, a vector norm $\|\mathbf{x}\|$ defined for \mathbf{x} is a non-negative number (i.e., a function $\mathbb{R}^n \rightarrow \mathbb{R}_+$) satisfying the following three axioms: 1/ $\|\mathbf{x}\| > 0$ when $\mathbf{x} \neq \mathbf{0}$ and $\|\mathbf{x}\| = 0$ iff $\mathbf{x} = \mathbf{0}$; 2/ $\|k\mathbf{x}\| = |k|\|\mathbf{x}\|$ for any scalar k and 3/ $\|\mathbf{x} + \mathbf{y}\| \leq \|\mathbf{x}\| + \|\mathbf{y}\|$. The most common norm is the L_2 norm or Euclidean norm, defined by $\|\mathbf{x}\|_2 = \sqrt{\sum_{k=1}^n |x_k|^2}$, where $|x_k|$ denotes the complex modulus or the absolute value. The L_1 norm of a complex vector \mathbf{x} is given by $\|\mathbf{x}\|_1 = \sum_{k=1}^n |x_k|$. The third classical norm to be consider here is the L_∞ which is defined by $\|\mathbf{x}\|_\infty = \max_{k,1 \leq k \leq n} |x_k|$. Given two real vectors \mathbf{x} and \mathbf{y} , the distance metric between the two points, denoted by $d(\mathbf{x}, \mathbf{y})$, is the mapping $d : \mathbb{R}^n \times \mathbb{R}^n \rightarrow \mathbb{R}_+$

which satisfies the following properties: 1/ non-negativity ($d(\mathbf{x}, \mathbf{y}) \geq 0$), identity ($d(\mathbf{x}, \mathbf{y}) = 0 \Leftrightarrow \mathbf{x} = \mathbf{y}$), commutativity ($d(\mathbf{x}, \mathbf{y}) = d(\mathbf{y}, \mathbf{x})$) and triangular inequality ($d(\mathbf{x}, \mathbf{z}) \leq d(\mathbf{x}, \mathbf{y}) + d(\mathbf{y}, \mathbf{z})$). In fact, a metric distance can be defined based on each vector norm proposed, hence the distance between two vectors is the norm of the difference, i.e. $d(\mathbf{x}, \mathbf{y}) = \|\mathbf{x} - \mathbf{y}\|$. The L_2 norm distance is the Euclidean distance. The L_1 and L_∞ norm distances are also called the Manhattan distance and the maximum distance, respectively. The Mahalanobis distance is a special case of the quadratic-form generalised distance metric in which the transform matrix is given by the covariance matrix Γ obtained from a training set of data that represents the reliability or scale of the measurement in each direction. The Mahalanobis distance between two vectors is given by $\|\mathbf{x} - \mathbf{y}\|_M = (\mathbf{x} - \mathbf{y})^T \Gamma^{-1} (\mathbf{x} - \mathbf{y})$. We remind that if \mathbf{x} and \mathbf{y} are n -dimensional vectors then the covariance matrix Γ is a $n \times n$ matrix. In the special case when all the vector components are statistically independent, but have unequal variances σ_k^2 , Γ is a diagonal matrix. In this case, the Mahalanobis distance reduces to $\|\mathbf{x} - \mathbf{y}\|_M = \sum_{k=1}^n \frac{(x_k - y_k)^2}{\sigma_k^2}$.

2.2 Color space representations

The first issue to be addressed in order to apply mathematical morphology to color images is the color space representation. The most direct way to manipulate digital color images is to work on the RGB color space (the usual sensors in digital cameras are RGB CCD's). A color image \mathbf{f} is a vector function $\mathbf{f}(\mathbf{x}) = (f_R(\mathbf{x}), f_G(\mathbf{x}), f_B(\mathbf{x})) \in \mathbb{Z}^3$, $\mathbf{x} \in \mathbb{Z}^2$, where $f_R(\mathbf{x})$, $f_G(\mathbf{x})$ and $f_B(\mathbf{x})$ are, respectively, the red, green, and blue channels at point \mathbf{x} .

However, the RGB color representation has some drawbacks: components are strongly correlated, lack of human interpretation, non uniformity, etc. A polar representation with the variables luminance, saturation et hue (lum/sat/hue) allows us to solve these problems. The HLS system is the most popular lum/sat/hue triplet. In spite of its popularity, the HLS representation (and another classical ones like HSV) often yields unsatisfactory results, for quantitative processing at least, because its luminance and saturation expressions are not norms, so average values, or distances, are falsified. In addition, these two components are not independent, which is a pity for a vector decomposition. The reader can find a comprehensive analysis of this question by Serra [16]. The drawbacks of the HLS system can be overcome by various alternative representations, according to different norms used to define the luminance and the saturation. The L_1 norm system has already been introduced in [15, 1] as follows:

$$\begin{cases} l = \frac{1}{3} (max + med + min) \\ s = \begin{cases} \frac{3}{2} (max - l) & \text{if } l \geq med \\ \frac{3}{2} (l - min) & \text{if } l \leq med \end{cases} \\ h = k \left[\lambda + \frac{1}{2} - (-1)^\lambda \frac{max+min-2med}{2s} \right] \end{cases}$$

where *max*, *med* and *min* refer the maximum, the median and the minimum of the RGB color

point (r, g, b) , k is the angle unit ($\pi/3$ for radians and 42 to work on 256 grey levels) and $\lambda = 0$, if $r > g \geq b$; 1, if $g \geq r > b$; 2, if $g > b \geq r$; 3, if $b \geq g > r$; 4, if $b > r \geq g$; 5, if $r \geq b > g$ allows to change to the colour sector. For each pixel, the luminance (or brightness) represents the total quantity of the intensity of light, the saturation represents a measurement of purity of the color, and the hue is an index representing the dominant wavelength (perceived color) of the light.

We would like also to compare it with the $L^*a^*b^*$ color space, the classical representation in colorimetry. The principal advantage of the $L^*a^*b^*$ space is its perceptual uniformity. However, the transformation from RGB to $L^*a^*b^*$ space is done by first transforming to the XYZ space, and then to the $L^*a^*b^*$ space [19]. The XYZ coordinates are depending on the device-specific RGB primaries and on the white point of illuminant. In most of situations, the illumination conditions are unknown and therefore a hypothesis must be made. We propose to choose the most common option: the CIE D_{65} daylight illuminant. The exact calculations are:

$$\begin{cases} L^* = \begin{cases} 116 \left(\frac{Y}{Y_n} \right)^{1/3} - 16 & \text{if } \frac{Y}{Y_n} > 0.008856 \\ 903.3 \left(\frac{Y}{Y_n} \right) & \text{if } \frac{Y}{Y_n} \leq 0.008856 \end{cases} \\ a^* = 500 \left[f \left(\frac{X}{X_n} \right) - f \left(\frac{Y}{Y_n} \right) \right] \\ b^* = 200 \left[f \left(\frac{Y}{Y_n} \right) - f \left(\frac{Z}{Z_n} \right) \right] \end{cases}$$

where $f \left(\frac{\alpha}{\alpha_n} \right) = \left(\frac{\alpha}{\alpha_n} \right)^{1/3}$ if $\frac{\alpha}{\alpha_n} > 0.008856$ or $f \left(\frac{\alpha}{\alpha_n} \right) = 7.787 \left(\frac{\alpha}{\alpha_n} \right) + \frac{16}{116}$ if $\frac{\alpha}{\alpha_n} \leq 0.008856$. The symbol α represents X , Y or Z , and XYZ are the tristimulus values of the sample, and X_n , Y_n and Z_n are the tristimulus values of the adapting reference white point, i.e., for D_{65} are $X_n = 0.950$; $Y_n = 1.000$; $Z_n = 1.089$. The L^* coordinate provides a correlate to perceived lightness. The a^* and b^* coordinates approximate respectively the red-green and yellow-blue of an opponent color space. Achromatic stimuli, such as whites, grays and blacks have values of 0 for both a^* and b^* .

Let $\mathbf{f} = (f_R, f_G, f_B)$ be a color image, its grey-level components in the improved LSH color space are (f_L, f_S, f_H) and in the $L^*a^*b^*$ color space are $(f_{L^*}, f_{a^*}, f_{b^*})$.

2.3 Color distances

Let $\mathbf{c}_k = (c_k^U, c_k^V, c_k^W)$ be the color point k in any generic color space UVW (e.g. in LSH $\mathbf{c}_k = (c_k^L, c_k^S, c_k^H)$). We can now define the color distance between two color vectors i and j as $\|\mathbf{c}_i - \mathbf{c}_j\|_{\Delta}^{UVW}$ where Δ is a particular metric. The four metric distances above recalled can be applied to color vectors according to the different color space representations, e.g. in RGB using L_2 we have $\|\mathbf{c}_i - \mathbf{c}_j\|_2^{RGB} = \sqrt{(c_i^R - c_j^R)^2 + (c_i^G - c_j^G)^2 + (c_i^B - c_j^B)^2}$. From the point of view of mathematical morphology, some

issues must be taken into account. The functions associated to the RGB components, to the $L^*a^*b^*$ components and to the luminance and saturation components of the LSH representation are complete totally ordered lattices. The hue should be considered as a special case. The hue component is an angular function defined on the unit circle \mathcal{C} , which has no partial ordering. For the hue, the angular difference [9, 6] is defined by $h_i \div h_j = |h_i - h_j|$ if $|h_i - h_j| \leq 180^\circ$ or $h_i \div h_j = 360^\circ - |h_i - h_j|$ if $|h_i - h_j| > 180^\circ$. Therefore, for all the color metric distances in LSH, the term associated to the hue must use the angular difference, e.g. $\|c_i - c_j\|_1^{LSH} = |c_i^L - c_j^L| + |c_i^S - c_j^S| + |c_i^H \div c_j^H|$. On the other hand, it is well known the instability of the hue component for the low saturation points (this is an important issue to build hue-based distances, gradients, ordering, etc.). In order to cope with this drawback, the different solutions are generally based on a weighting of the hue by the saturation [3, 5, 2]. We propose to use the simplest technique, multiplying the angular difference by the average saturation, i.e. $\frac{(c_i^S + c_j^S)}{2} |c_i^H \div c_j^H|$. As suggested in [3], other more sophisticated saturation-based weighing functions can be applied (e.g. sigmoid). Moreover, concerning the hue component manipulation, it is possible to fix an origin on the unit circle, denoted by h_0 . We can define now a h_0 -centered hue function by computing for each point i the value $(h_i \div h_0)(x) = h_i(x) \div h_0$. This function $(h_i \div h_0)(x)$ is an ordered set and therefore leads to a complete totally ordered lattice.

Before applying these color distances to define morphological operators, a relevance analysis of the alternative distances shall be made. Firstly, the L_∞ norm distances could cause serious artefacts in the filtered color images because color vectors will be ordered according to only one of the components which can change for a set of points. We can suppose that the results according to L_1 or L_2 will be relatively similar. In fact, the Mahalanobis distance can be interpreted as a generalisation of them with the advantage of setting different weights for the components. Moreover, for the sake of simplicity of this paper, we consider that in the three color representations the components are statistically independent and we can rewrite the Mahalanobis distance as a weighting distance, i.e., $\|c_i - c_j\|_{M(\omega_1, \omega_2, \omega_3)}^{UVW} = \omega_1(c_i^U - c_j^U)^2 + \omega_2(c_i^V - c_j^V)^2 + \omega_3(c_i^W - c_j^W)^2$.

3 Distances-based morphological color operators

We have previously study in depth the extension of morphological operators to color images based on lexicographical cascades from a LSH representation in norm L_1 [1, 2]. The rationale behind the approach here developed is more ambitious, proposing a generic framework valid for any color representation and adding the flexibility of a “reference color”-based morphology. In fact, after defining as reference the maximum gray value, the grayscale morphology can be interpreted in terms of distances to this refer-

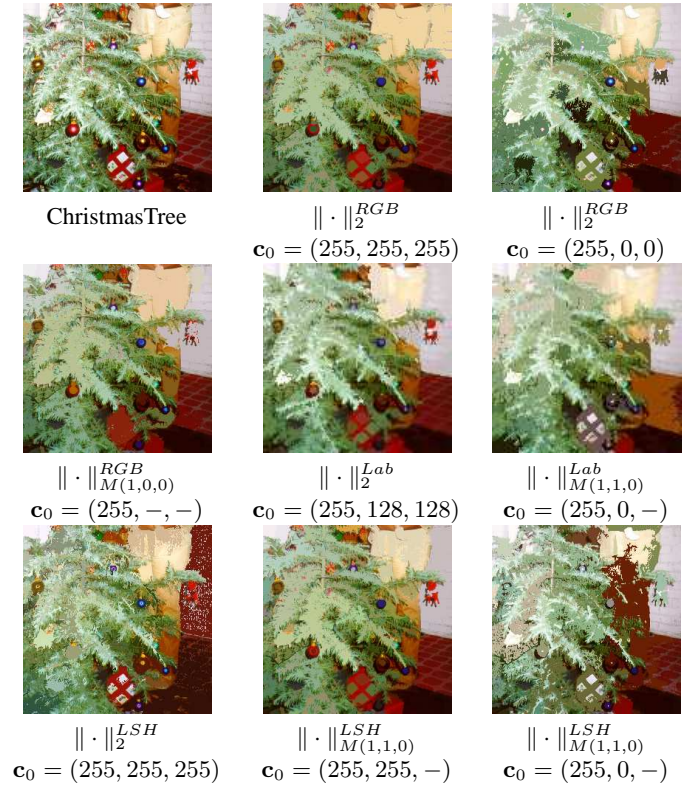


Figure 1. Comparison of color opening by reconstruction $\gamma_\Omega(\mathbf{f})$ for the image \mathbf{f} “ChristmasTree” (the marker is an erosion $\varepsilon_{\Omega, nB}(\mathbf{f})$ where the structuring element B is a square of size $n = 20$) according to different distance-based total orderings.

ence: the dilatation δ tends to move toward this reference (i.e. δ is the value which have minimal distance to the reference within the structuring element) and the erosion ε away from it (i.e. ε is the value with maximal distance). This paradigm is directly applicable to color images (after fixing the color representation, the reference color c_0 and the color distance $\|\cdot\|$) by defining the following ordering for two color points: $c_i < c_j \Leftrightarrow \|c_i - c_0\| > \|c_j - c_0\|$. But this is only a partial ordering, i.e., two or more distinct color vectors within the structuring element can be equidistant from the reference. In order to have a total ordering we propose to complete this primary reduced ordering with a lexicographical cascade.

3.1 Total orderings using distances completed with lexicographical cascades

The Ω -ordering or $<_{\Omega}$ is defined as: $\mathbf{c}_i <_{\Omega} \mathbf{c}_j$ iff

$$\left\{ \begin{array}{l} \|\mathbf{c}_i - \mathbf{c}_0\|_{\Delta}^{UVW} > \|\mathbf{c}_j - \mathbf{c}_0\|_{\Delta}^{UVW} \text{ or} \\ \|\mathbf{c}_i - \mathbf{c}_0\|_{\Delta}^{UVW} = \|\mathbf{c}_j - \mathbf{c}_0\|_{\Delta}^{UVW} \text{ and} \\ \left\{ \begin{array}{l} c_i^V < c_j^V \text{ or} \\ c_i^V = c_j^V \text{ and } c_i^U < c_j^U \text{ or} \\ c_i^V = c_j^V \text{ and } c_i^U = c_j^U \text{ and } c_i^W < c_j^W \end{array} \right. \end{array} \right.$$

We denote compactly this lexicographical cascade by $\Omega_{\Delta, \mathbf{c}_0}^{UVW} \vdash (V \rightarrow U \rightarrow W)$. In this case, the priority is given to the component V , then to U and finally to W . Obviously, it is possible to define other orders for imposing a dominant role to any other of the vector components. To simplify the number of alternatives, and based on the best results obtained from our previous works on lexicographical cascades, we propose to fix the ordering of the components for the three color spaces representations as follows: 1) $\vdash (G \rightarrow R \rightarrow B)$, 2) $\vdash (L \rightarrow S \rightarrow -(H \div h_0))$ (the origin of the hues correspond is the same as for \mathbf{c}_0) and 3) $\vdash (L \rightarrow a \rightarrow b)$.

3.2 Morphological color operators

Once these orderings have been established, the morphological color operators are defined in the standard way. We limit our developments to the flat operators [12]. The *color erosion* of an image \mathbf{f} at pixel x by the structuring element B of size n is $\varepsilon_{\Omega, nB}(\mathbf{f})(x) = \{\mathbf{f}(y) : \mathbf{f}(y) = \inf_{\Omega}[\mathbf{f}(z)], z \in n(B_x)\}$, where \inf_{Ω} is the infimum according to the total ordering Ω . The corresponding *color dilation* $\delta_{\Omega, nB}$ is obtained by replacing the \inf_{Ω} by the \sup_{Ω} , i.e., $\delta_{\Omega, nB}(\mathbf{f})(x) = \{\mathbf{f}(y) : \mathbf{f}(y) = \sup_{\Omega}[\mathbf{f}(z)], z \in n(B_x)\}$. A *color opening* is an erosion followed by a dilation, i.e., $\gamma_{\Omega, nB}(\mathbf{f}) = \delta_{\Omega, nB}(\varepsilon_{\Omega, nB}(\mathbf{f}))$, and a *color closing* is a dilation followed by an erosion, i.e., $\varphi_{\Omega, nB}(\mathbf{f}) = \varepsilon_{\Omega, nB}(\delta_{\Omega, nB}(\mathbf{f}))$. Once the color opening and closing are defined it is obvious how to extend other classical operators like the *alternate sequential filters*, i.e. $ASF(\mathbf{f})_{\Omega, nB} = \varphi_{\Omega, nB} \gamma_{\Omega, nB} \cdots \varphi_{\Omega, 2B} \gamma_{\Omega, 2B} \varphi_{\Omega, B} \gamma_{\Omega, B}(\mathbf{f})$. Moreover, using a color distance (which can be different of the distance associated to the ordering Ω) to calculate the image distance d , given by difference point-by-point of two color images $d(x) = \|\mathbf{f}(x), \mathbf{g}(x)\|$, we can easily define the *morphological gradient*, i.e., $\varrho_{\Omega}(\mathbf{f}) = \|\delta_{\Omega, B}(\mathbf{f}), \varepsilon_{\Omega, B}(\mathbf{f})\|$, and the *top-hat transformation*, i.e., $\rho_{\Omega, nB}^+(\mathbf{f}) = \|\mathbf{f}, \gamma_{\Omega, nB}(\mathbf{f})\|$. In addition, we propose also the extension of the operators “by reconstruction” implemented using the *color geodesic dilation* which is based on restricting the iterative dilation of a function marker \mathbf{m} by B to a function reference \mathbf{f} [18], i.e., $\delta_{\Omega}^n(\mathbf{m}, \mathbf{f}) = \delta_{\Omega}^1 \delta_{\Omega}^{n-1}(\mathbf{m}, \mathbf{f})$, where $\delta_{\Omega}^1(\mathbf{m}, \mathbf{f}) = \delta_{\Omega, B}(\mathbf{m}) \wedge_{\Omega} \mathbf{f}$. The *color reconstruction* by dilation is defined by $\gamma_{\Omega}^{rec}(\mathbf{m}, \mathbf{f}) = \delta_{\Omega}^i(\mathbf{m}, \mathbf{f})$, such that $\delta_{\Omega}^i(\mathbf{m}, \mathbf{f}) = \delta_{\Omega}^{i+1}(\mathbf{m}, \mathbf{f})$ (idempotence).

In figure 1 is given a comparison of the results obtained for a color opening by reconstruction $\gamma_{\Omega}(\mathbf{f})$ of the image “ChristmasTree”. As we can observe, the results are absolutely different according to the distance-based total ordering chosen. We show only examples for the L_2 and the Mahalanobis distance. As we have expected, the orderings based on L_{∞} yield to very unsatisfactory visual results and the results for L_1 norm distances are almost equal to ones for L_2 . Note also the flexibility of the approach, for instance, in RGB the result of the opening for L_2 distance to the origin (255, 0, 0) (pure red), which suppresses all the small red objects, is very different of the Mahalanobis distance with weights (1, 0, 0) (the R component is exclusively considered) to the same origin. On the other hand, we can observe that the orderings with distances including chromatic components (i.e. h, a* and b*) produce poor results. Moreover the choice of the origin is not easily understandable for the a* and b* components. Even if the Euclidean distance in the $L^*a^*b^*$ color space has interesting perceptual properties, we can remark that for the implementation of morphological operators the most important issue is in fact the choice of the origin. Hence, the use of the L_2 distance in LSH or $L^*a^*b^*$ should be considered for feature extraction operators according to a specific reference color. We can remark also that, in order to filter in a general way the structures of a natural color image, the opening to remove all the bright objects is visually better for $\|\cdot\|_2^{RGB}$, $\mathbf{c}_0 = (255, 255, 255)$ than for $\|\cdot\|_{M(1,1,0)}^{LSH}$, $\mathbf{c}_0 = (255, 255, -)$. The luminance and saturation components allow us therefore a better control of the significant components than the RGB components.

4 Color enhancement by means of contrast mappings

The contrast mapping is a particular operator from a more general class of transformations called toggle mappings [13]. A contrast mapping is defined, on the one hand, by two primitives ϕ_1 and ϕ_2 applied to the initial function, and on the other hand, by a decision rule which makes, at each point x the output of this mapping toggles between the value of ϕ_1 at x and the value of ϕ_2 according to which is closer to the input value of the function at x . If the primitives are an erosion $\varepsilon_{\Omega, nB}(\mathbf{f})$ and the dual dilation $\delta_{\Omega, nB}(\mathbf{f})$, the *color contrast mapping* for an image \mathbf{f} is given by [7]:

$$\kappa_{\Omega, nB}^{\varepsilon \delta}(\mathbf{f})(x) = \begin{cases} \delta_{\Omega, nB}(\mathbf{f})(x) & \text{if } \|\mathbf{f}(x) - \delta(\mathbf{f})(x)\| \leq \|\mathbf{f}(x) - \varepsilon(\mathbf{f})(x)\| \\ \varepsilon_{\Omega, nB}(\mathbf{f})(x) & \text{if } \|\mathbf{f}(x) - \delta(\mathbf{f})(x)\| > \|\mathbf{f}(x) - \varepsilon(\mathbf{f})(x)\| \end{cases}$$

This morphological transformation enhances the local contrast of \mathbf{f} by sharpening its edges. It is usually applied not only once but is iterated, and the iterations converge to a limit reached after a finite number of iterations.

Another interesting color contrast mapping $\kappa_{\Omega, nB}^{\gamma \varphi}(\mathbf{f})$ is defined by changing in the previous expression the pair of

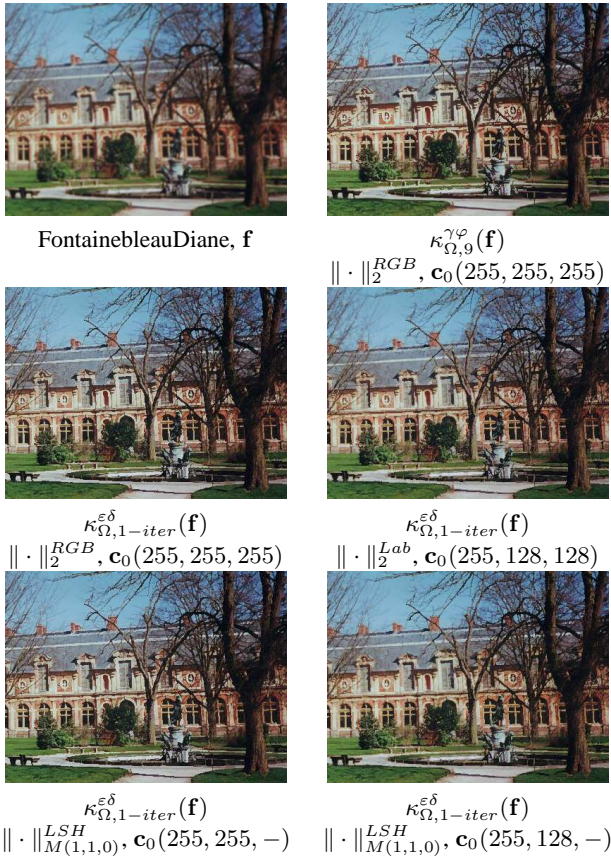


Figure 2. Contrast enhancement of color image \mathbf{f} “FontainebleauDiane” using a contrast mapping κ according to different distance-based total ordering.

erosion/dilation by an opening $\gamma_{\Omega, nB}(\mathbf{f})$ and the dual closing $\varphi_{\Omega, nB}(\mathbf{f})$ [8]. This second contrast operator is idempotent. More recently, these sharpening methods are called shock filters [10].

Figure 2 shows a comparative example of contrast enhancement of the blurred image (using a Gaussian $\sigma = 5$) “FontainebleauDiane” by means of contrast mappings. It is well known that, in order to have significant enhancement, the size of $\kappa^{\gamma\varphi}$ must be considerable and that can involve visual artefacts. In fact, the effects obtained are better for the iteration of $\kappa^{\epsilon\delta}$. Concerning the distance-based total ordering, it seems that the best visual result is associated to $\|\cdot\|_{M(1,1,0)}^{LSH}, \mathbf{c}_0(255, 128, -)$, which enhances the bright/dark structures, with an intermediate saturation (chromatic and achromatic simultaneously) and independently of the hue.

5 Color noise suppression using morphological centre

The opening/closing are nonlinear smoothers filters, and classically an opening followed by a closing (or a closing followed by an opening) can be used to suppress impulse

noise, i.e., suppressing positive spikes via the opening and negative spikes via the closing and without blurring the contours. However the results are usually not satisfactory. A more interesting operator to suppress noise is the morphological centre, called also automedian filter [12, 13].

Given an opening $\gamma_{\Omega}(\mathbf{f})$ and the dual closing $\varphi_{\Omega}(\mathbf{f})$ with a small structuring element (typically square of size equal to the “noise size”), the *color morphological centre* associated to these primitives for an image \mathbf{f} is given by the algorithm:

$$\zeta_{\Omega}(\mathbf{f}) = [f \vee_{\Omega}(\gamma\varphi\gamma(\mathbf{f}) \wedge_{\Omega} \varphi\gamma\varphi(\mathbf{f}))] \wedge_{\Omega}(\gamma\varphi\gamma(\mathbf{f}) \vee_{\Omega} \varphi\gamma\varphi(\mathbf{f})).$$

This is an increasing and autodual operator, not idempotent, but the iteration of ζ presents a point monotonicity and converges to the idempotence, i.e. $\widehat{\zeta}_{\Omega}(\mathbf{f}) = [\zeta_{\Omega}(\mathbf{f})]^i$, such that $[\zeta]^i = [\zeta]^{i+1}$.

In figure 3 is given an example of application of morphological centre to filter color noise. The image “CarmenBianca” has been corrupted by adding salt-and-pepper noise on the hue component (occurring with probability 0.05) and where the luminance for noise pixels is maximal and the saturation is half. As we can observe, for this noise distribution, the results are again better using only the luminance component ($\|\cdot\|_{M(1,0,0)}^{LSH}, \mathbf{c}_0(255, -, -)$) than the RGB components ($\|\cdot\|_2^{RGB}, \mathbf{c}_0(255, 255, 255)$). Note also that the result associated to the open-closing operator for a size equal to the centre is worse in terms of noise suppression. However the best result is for $\|\cdot\|_{M(1,1,0)}^{LSH}, \mathbf{c}_0(255, 128, -)$ which corresponds to the noise distribution properties. In fact, it seems that the flexible choice of a particular distance and a color reference can be interesting in order to obtain optimal filters for a particular distribution of noise. The challenge lies in the estimation of the statistical color noise properties, then the Mahalanobis distance is naturally well adapted to this kind of problems (applying a estimated covariance matrix Γ).

6 Conclusions and perspectives

We have introduced in this study an algorithmic framework to apply, in a reliable and generic way, mathematical morphology operators to color images. The methodology is based on a R-ordering (using the distance to a reference color) completed by a C-ordering (using a lexicographical cascade). We have shown the interest of the approach for two filtering applications (denoising and enhancement). Other applications, such as feature extraction, are at present under development. This framework could be also valid to develop other rank-based operators like color median filters. Moreover, the approach is also well adapted to other multivariate data problems, for instance, morphological processing of hyperspectral images.

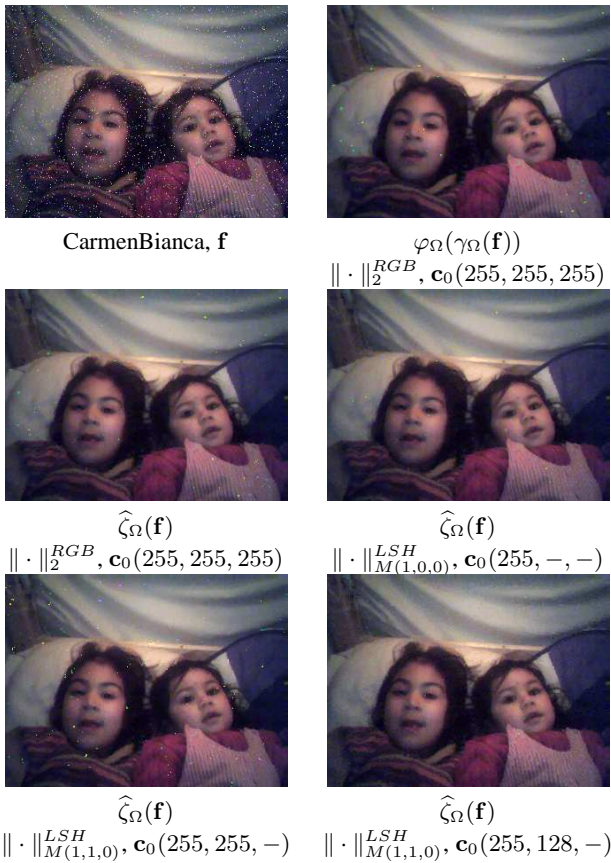


Figure 3. Denoising of color image f ‘‘CarmenBianca’’ using a morphological centre $\hat{\zeta}$ according to different distance-based total ordering.

References

[1] J. Angulo, *Morphologie mathématique et indexation d’images couleur. Application à la microscopie en biomédecine*. Ph.D. Thesis, Ecole des Mines, Paris, December 2003.

[2] J. Angulo, Unified morphological color processing framework in a lum/sat/hue representation, in *Proc. of International Symposium on Mathematical Morphology (ISMM ’05)*, Kluwer, 2005, 387–396.

[3] T. Carron and P. Lambert, Color edge detector using jointly Hue, Saturation and Intensity, in *Proc. of IEEE International Conference on Image Processing (ICIP’94)*, 1994, pp. 977–981.

[4] J. Goutsias, H.J.A.M. Heijmans and K. Sivakumar, Morphological Operators for Image Sequences, *Computer Vision and Image Understanding*, 62(3) (1995) 326–346.

[5] A. Hanbury and J. Serra, Mathematical morphology in the HLS colour space, in *Proc. 12th British*

Machine Vision Conference (BMV’01), Manchester, 2001, pp. II-451–460.

[6] A. Hanbury and J. Serra, Morphological Operators on the Unit Circle, *IEEE Transactions on Image Processing*, 10(12) (2001) 1842–1850.

[7] H. Kramer and J. Bruckner, Iterations of non-linear transformations for enhancement on digital images, *Pattern Recognition*, 7, 1975, 53–58.

[8] F. Meyer and J. Serra, Contrasts and activity lattice, *Signal Processing*, 16, 1989, 303–317.

[9] R.A. Petters II, Mathematical morphology for angle-valued images, in *Proc. of Non-Linear Image Processing VIII*, 1997, Vol. SPIE 3026, 84–94.

[10] S. Osher, L.I. Rudin, Feature-oriented image enhancement using shock filters, *SIAM Journal of Numerical Analysis*, 27, 1990, 919–940.

[11] L.J. Sartor and A.R. Weeks, Morphological operations on color images, *Electronic imaging*, 2001, Vol. 10(2), 548–559.

[12] J. Serra, *Image Analysis and Mathematical Morphology. Vol I, and Image Analysis and Mathematical Morphology. Vol II: Theoretical Advances*, London: Academic Press, 1982,1988.

[13] J. Serra, Toggle mappings, in (Simon, Ed.) *From Pixels to Features*, 1989, North Holland, Amsterdam, 61–72.

[14] J. Serra, Anamorphoses and Function Lattices (Multi-valued Morphology), in (Dougherty, Ed.) *Mathematical Morphology in Image Processing*, 1992, Marcel-Dekker, 483–523.

[15] J. Serra, Espaces couleur et traitement d’images, *CMM-Ecole des Mines de Paris*, Internal Note N-34/02/MM, October 2002, 13 p.

[16] J. Serra, Morphological Segmentation of Colour Images by Merging of Partitions, in *Proc. of International Symposium on Mathematical Morphology (ISMM ’05)*, Kluwer, 2005, 151–176.

[17] H. Talbot, C. Evans and R. Jones, Complete ordering and multivariate mathematical morphology: Algorithms and applications, in *Proc. of the International Symposium on Mathematical Morphology (ISMM’98)*, Kluwer, 1998, 27–34.

[18] L. Vincent, Morphological Grayscale Reconstruction in Image Analysis: Applications and Efficient Algorithms, *IEEE Transactions on Image Processing*, Vol. 2(2), 1993, 176–201.

[19] G. Wysecki and W.S. Stiles, *Color Science : Concepts and Methods, Quantitative Data and Formulae*, 2nd edition. John Wiley & Sons, New-York, 1982.